# Direct Imaging of the Electrochemical Deposition of Poly(3,4-ethylenedioxythiophene) by Transmission Electron Microscopy

Jinglin Liu,[†,‡] Bin Wei,[†,‡] Jennifer D. Sloppy,[‡] Liangqi Ouyang,[‡,§] Chaoying Ni,[‡] and David C. Martin*[,‡,||]

[‡]Materials Science and Engineering and [||]Biomedical Engineering, The University of Delaware, Newark, Delaware 19716, United States

S Supporting Information

ABSTRACT: Conjugated polymers are electronically and ionically active organic materials of interest for use in a variety of devices. Electrochemical deposition is a convenient method for precisely fabricating conjugated polymer thin films, yet a detailed, quantitative understanding of nucleation and growth mechanisms has remained elusive. Here, we report direct imaging of the in situ electrochemical deposition of poly(3,4-ethylenedioxythiophene) (PEDOT) from an aqueous solution of EDOT monomer using Transmission Electron Microscopy with an electrochemical liquid flow cell. We found that PEDOT deposition began preferentially at the edge of the glassy carbon anodes at the beginning of the reaction. Fluctuating clusters of liquid-like oligomers were observed to form near the electrode surfaces. As the reaction continued, both the nucleation of new domains as well as the growth of pre-existing PEDOT deposits were observed, leading to systematic increases in film thickness and roughness.
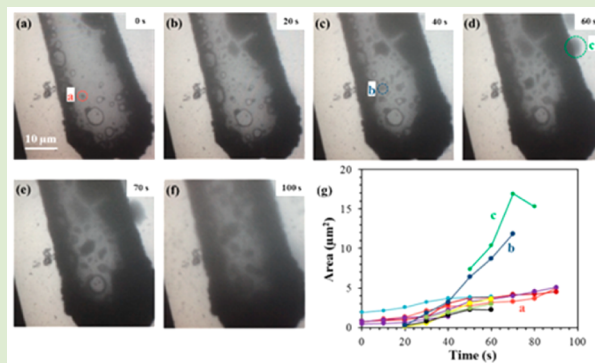
Conjugated polymers have received considerable interest for a variety of applications including photovoltaic cells, organic light emitting diodes, sensors, and biomedical devices.[1−5] These materials can be synthesized via oxidative chemical polymerization or electrochemical deposition. Electrochemical techniques are especially suitable for synthesizing thin films because the reaction conditions can be precisely controlled.[6,7] There have been many studies on the structural, chemical, and electrochemical properties of electrodeposited conjugated polymer films.[8,9] However, a quantitative understanding of the details of the process remains elusive. Early stage electrochemical deposition of conjugated polymers has been studied by lower resolution or indirect methods such as cyclic voltammetry, impedance spectroscopy, UV−vis spectroscopy, and atomic force microscopy (AFM).[10−13] However, the results have not provided a detailed understanding of the nucleation and growth mechanisms and corresponding relationships between film structure and properties. Direct imaging of the process by high-resolution electron microscopy is a potential method for answering some of these open questions. Previous studies have shown that it is feasible to investigate the kinetics of inorganic solid nucleation and growth from precursor liquid solutions using specially designed electrochemical liquid cells inside a transmission electron microscope (TEM). Radisic and co-workers performed a quantitative study of the electrochemical nucleation and growth of nanoscale copper clusters.[14] Regan reported the electrochemical deposition of lead from an aqueous solution of lead(III) nitrate.[15] Recently, Sacci reported the direct visualization of solid electrolyte interface morphology and growth kinetics during

lithium deposition.[16] However, the direct in situ observation of electrochemical deposition of organic conjugated polymers has never been reported before. One major difficulty in successfully imaging the in situ deposition of organic polymeric materials is the control of electron beam dose. Inorganic materials have a relatively high tolerance to the electron beam, and are thus more readily imaged by TEM. However, as is typical for organic materials, conjugated polymers are fairly sensitive to electron beam irradiation, and thus, particular care is needed to monitor and control the dose used during imaging. We have previously reported direct imaging of the diacetylene solid-state monomer−polymer phase transformation using low dose TEM and electron diffraction.[17] Recently, Schneider has carefully examined the interactions between high-energy electrons and irradiated medium for liquid cell electron microscopy.[18] With the emerging development of electrochemical liquid flow cells[19−21] along with the careful control of beam dose, we show here that it is indeed feasible to accomplish the in situ electrochemical deposition of conjugated polymers in the TEM.

In this letter, we report for the first time the in situ electrochemical deposition of PEDOT films from aqueous solution with liquid flow cell TEM. The microstructural evolution during the electrochemical polymerization was carefully monitored in situ, providing information about the

nature of PEDOT nucleation and growth. These local mechanistic insights have provided unprecedented detail about the deposition process. We expect that continued systematic studies of the growth mechanisms from different deposition conditions, monomer chemistries, and secondary components in the reaction mixture will make it possible to precisely tailor and optimize the structure and properties of electrochemically deposited conjugated polymers.

PEDOT is one of the most promising and widely used conjugated polymers due to its excellent conductivity and high chemical stability.[22] The in situ observation of PEDOT deposition was performed in a specially designed, commercially available liquid flow cell that can tolerate the high vacuum and also fits into the limited space inside the pole piece of a conventional TEM.[23] The liquid cell used two microfabricated silicon chips (a top electrochemical chip and bottom spacer chip) with a three-electrode design to enable voltage control and current measurements. Liquid flowed through channel with a thickness defined by the size of the spacers on the bottom chip (here 500 nm). Thin (50 nm) electron transparent silicon nitride membranes on both chips allowed electrons to pass through the liquid for in situ TEM imaging. Figure S1 shows Scanning Electron Microscopy (SEM) images of the top electrochemical chip. There was a 20 μm wide glassy carbon working electrode (WE) in the middle of the silicon nitride viewing window (200 μm × 40 μm). The platinum counter electrode (CE) was 100 μm wide, located 500 μm away from the WE. There was also a 10 μm wide platinum reference electrode (RE) that followed the shape of the WE and was placed 90 μm away from the WE. The in situ experiments were conducted on a 300 kV JEOL 3010 TEM. An aqueous solution containing 0.01 M EDOT and 0.10 M LiClO$_4$ as the supporting electrolyte was used in continuous flow mode at a rate of 2 μL/ min.[10] During the experiment, the first few CV cycles were run on the bench to verify effective electrical contact. The liquid cell was then transferred into the TEM column to continue further in situ deposition. The in situ growth of PEDOT in the TEM at the electrode surface in the presence of LiClO$_4$ was carried out at constant voltage (potentiostatic) conditions at +1.00 and +1.20 V versus the platinum reference electrode. The brightness of the beam was estimated at 0.05−5 μA/cm^2, and the total exposure times were ~30 min from electron beam on until the final round of potentiostatic deposition. This corresponds to total doses of 0.1−1 mC/cm^2, which were substantially below the characteristic doses necessary to cause significant beam damage in PEDOT (~0.1 C/cm^2).[5] The bright field TEM images in Figure 1 are examples of in situ deposited PEDOT imaged at an early stage (Figure 1a, after initial 10 CV scans from −0.60 V to +1.20 V) and a later stage (Figure 1b, after subsequent constant voltage deposition of +1.00 V for 3 min and +1.20 V for 5 min) of the process. These PEDOT films were deposited directly onto glassy-carbon working electrodes (WE) supported on electron transparent silicon nitride membranes.

The surface roughness and mass thickness of PEDOT films increased during the electrochemical polymerization (Figures 1 and 2). The PEDOT initially deposited preferentially near the edges of the working electrodes where the electric field was the highest. With further electrochemical deposition, PEDOT nucleation and growth took place on the center of the glassy carbon electrodes as well. The TEM images showed that the sizes of PEDOT clusters ranged from hundreds of nanometers to several microns. As the deposition continued, the film
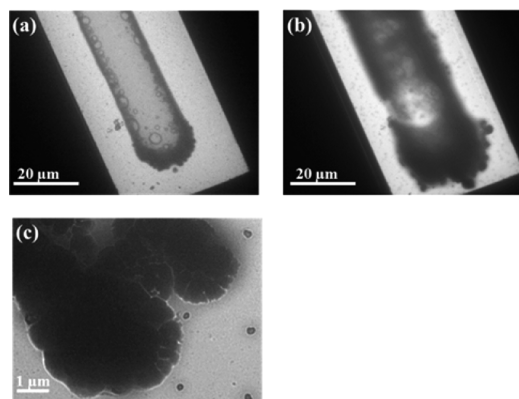

Figure 1. Bright field TEM images of in situ electrochemical deposition of PEDOT: (a) Early stage in the process (right after initial CV deposition on bench) showing the dark PEDOT depositing from an aqueous solution onto a 20 μm wide glassy carbon working electrode (anode) supported on a thin silicon nitride membrane; (b) Later stage in the process (after subsequent constant voltage deposition), showing the increased thickness and formation of rough protrusions at the edge of the PEDOT film; (c) Higher magnification view of the rough edge of the PEDOT film after further deposition.
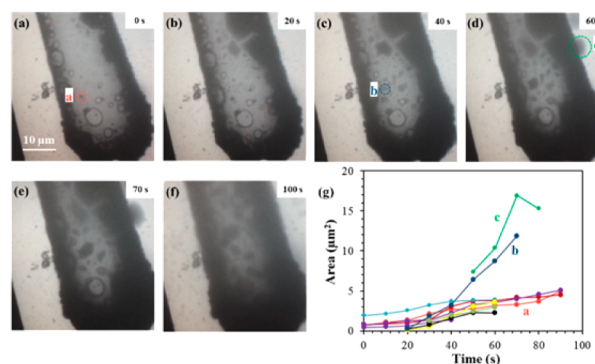

Figure 2. Growth of PEDOT clusters during electrochemical deposition. (a−f) Captured frames from live video recording of in situ PEDOT deposition under TEM at constant voltage of +1.20 V; (g) Projected areas of individual PEDOT clusters measured from the video.

thickened and the edges became rougher. The edges of the film show new PEDOT clusters of 500 nm or less that have formed around preexisting PEDOT clusters during further polymerization (Figure 1c), leading to rougher edges. Similar rough structures have often been seen in previous experiments.[24−26] Mass thickness contrast fluctuations from dark fluid domains with a typical size of several hundreds of nanometers were observed near the electrode−solution interface in video recordings taken during the process (Figure 2). These domains presumably correspond to local droplets of liquid enriched in the PEDOT oligomers that are formed during the electrochemical deposition process. The liquid-like nature of these fluctuating domains was verified by continuous flow of the electrolyte in the reaction cell (such as cluster "c" in Figure 2). The ring-shaped structures seen on the solid films in TEM are evidently due to the solidification and precipitation of solid PEDOT clusters from these oligomer-rich fluid droplets onto the WE surface. To our knowledge, this is the first time that the imaging of this transformation from liquid EDOT monomer and PEDOT oligomers to solid PEDOT polymer has been directly observed. This solidification and precipitation process

also provides a reasonable explanation for the common "bumpy" surface morphology of electrochemically deposited PEDOT films usually observed in the SEM or AFM.[5,26]

The PEDOT oligomer clusters nucleated in what appeared to be an essentially random fashion on the center of the electrode. Once two adjacent clusters met each other, they merged into a larger cluster and the growth continued around the new cluster. The total number of PEDOT clusters initially increased as the deposition continued, starting with approximately 10 small clusters in an area of 200 μm^2 and gradually increasing to around 30 clusters in 15 s. At the same time, previously formed PEDOT clusters increased in both their mass thickness and size. Shown in Figure 2g is the growth of several individual PEDOT clusters with a few of the characteristic clusters labeled in the image. It was found that the size of the PEDOT clusters did not increase at a constant rate, but rather in a somewhat irregular fashion. During a given time interval, some clusters grew quickly, whereas others were evidently more dormant. These variations are presumably due to local variations in the rate of nucleation and growth of additional PEDOT.[10,24] We also saw certain clusters occasionally decrease in size (such as cluster "c" between 70 and 100 s), presumably because they were still somewhat liquid-like in nature and thus able to be removed by the continued flow of liquid in the cell.[27]

After the electropolymerization of PEDOT in TEM, the electrochemical chip was taken out for examination by optical microscopy (OM), SEM, and Energy-Dispersive X-ray Spectroscopy (EDS). In Figure 3, OM of the electrochemical top
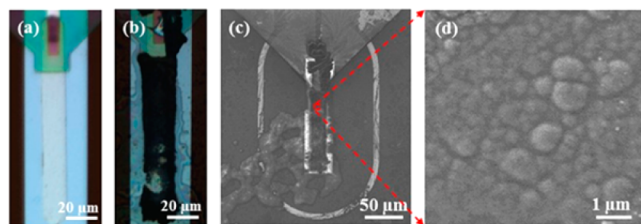

Figure 3. Optical and SEM images after electrochemical deposition: (a) Optical micrograph before deposition showing bare working electrode; (b) Optical micrograph after deposition showing accumulated dark PEDOT on the working electrode; (c) SEM image after deposition; (d) Higher magnification SEM image showing the "bumpy" surface morphology of the deposited PEDOT film.

chip before deposition (Figure 3a) showed the transparent glassy carbon WE over the silicon nitride viewing window. After electrochemical deposition (Figure 3b), PEDOT deposition with its characteristic dark color was observed on the WE. The SEM pictures (Figure 3c,d) confirmed the "bumpy" surface morphology commonly observed in electrochemically deposited PEDOT films.[5,26]

To confirm the elemental composition of the deposited thin film, EDS mapping was performed. As shown in Figure 4b, the sulfur signal characteristic of the PEDOT overlapped with the dark rough material formed on the glassy carbon WE. The elemental mapping results for carbon (Figure 4c, from PEDOT and WE), chlorine (Figure 4d, from the counterion), and oxygen (Figure 4e, from both PEDOT and counterion) all corresponded well with their expected distribution. We also saw the expected distribution of silicon (Figure 4f) from the microfabricated substrate.
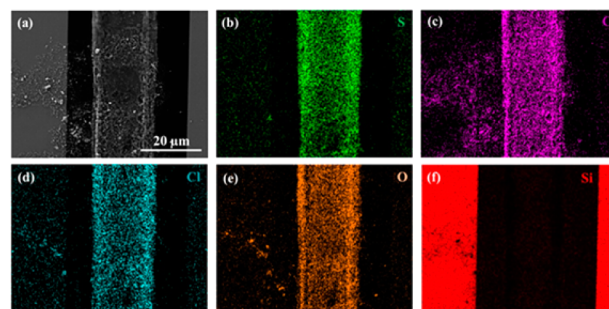

Figure 4. EDS elemental mapping after in situ electrochemical deposition of PEDOT: (a) Secondary electron image; (b) Sulfur (PEDOT); (c) Carbon (PEDOT and glassy carbon working electrode); (d) Chlorine (perchlorate dopant); (e) Oxygen (PEDOT and perchlorate dopant); (f) Silicon (microfabricated substrate).

In this study, we have demonstrated the direct in situ electrochemical deposition of organic materials in the TEM. The PEDOT clusters forming during deposition were directly imaged and novel details of the deposition process were observed for the first time. At first, electrochemical deposition of PEDOT occurred preferentially at the edge of glassy carbon WE. As deposition continued, subsequent PEDOT clusters formed on the center of the electrode, and both the surface roughness and mass thickness of PEDOT films increased. Liquid-like fluctuating domains were observed near the reaction interface during the polymerization process. The growth of the PEDOT domains was irregular, with variations in growth rate seen for individual clusters as the reaction continued. These local mechanistic insights make it possible for us to investigate the electrochemical deposition of conjugated polymers in much more detail. With this better understanding of the nucleation and growth mechanisms, new molecular designs and electrochemical deposition methods for better device performance are expected. For example, we should now be able to examine the role of other components that can be added to the mixture to tailor the morphology and properties of the film, including hydrogels, dissolvable fibers or particles, or even biological components, such as living cells.

■ ASSOCIATED CONTENT

Ⓢ Supporting Information

■ AUTHOR INFORMATION

Corresponding Author
*E-mail: milty@udel.edu.

Present Address
§Biomolecular and Organic Electronics, IFM, Linkoping University, Linkoping, Sweden.

Author Contributions
†These authors contributed equally to the manuscript (J.L. and B.W.).

Notes
The authors declare the following competing financial interest(s): D.C.M. is a Co-Founder and Chief Scientific

Officer for Biotectix LLC (www.biotectix.com), a University of Michigan spin-off company developing electronically and ionically active conjugated polymer-based coatings for interfacing biomedical devices with living tissue.

■ REFERENCES

(1) Vohra, V.; Kawashima, K.; Kakara, T.; Koganezawa, T.; Osaka, I.; Takimiya, K.; Murata, H. *Nat. Photonics* **2015**, *9*, 403.

(2) Hoffmann, S. T.; Jaiser, F.; Hayer, A.; Bässler, H.; Unger, T.; Athanasopoulos, S.; Neher, D.; Köhler, A. *J. Am. Chem. Soc.* **2013**, *135*, 1772.

(3) Beaujuge, P. M.; Reynolds, J. R. *Chem. Rev.* **2010**, *110*, 268.

(4) Ji, X.; Yao, Y.; Li, J.; Yan, X.; Huang, F. *J. Am. Chem. Soc.* **2013**, *135*, 74.

(5) Martin, D. C.; Wu, J.; Shaw, C. M.; King, Z.; Spanninga, S. A.; Richardson-Burns, S.; Hendricks, J.; Yang. *Polym. Rev.* **2010**, *50*, 340.

(6) Feldman, K. E.; Martin, D. C. *Biosensors* **2012**, *2*, 305.

(7) Groenendaal, L.; Zotti, G.; Aubert, P.-H.; Waybright, S. M.; Reynolds, J. R. *Adv. Mater.* **2003**, *15*, 855.

(8) Mortimer, R. J. *Annu. Rev. Mater. Res.* **2011**, *41*, 241.

(9) King, Z.; Shaw, C. M.; Spanninga, S. A.; Martin, D. C. *Polymer* **2011**, *52*, 1302.

(10) Randriamahazaka, H.; Noël, V.; Chevrot, C. *J. Electroanal. Chem.* **1999**, *472*, 103.

(11) Hillman, A. R.; Mallen, E. F. *J. Electroanal. Chem. Interfacial Electrochem.* **1988**, *243*, 403.

(12) Innocenti, M.; Loglio, F.; Pigani, L.; Seeber, R.; Terzi, F.; Udisti, R. *Electrochim. Acta* **2005**, *50*, 1497.

(13) Arteaga, G. C.; del Valle, M. A.; Antilén, M.; Romero, M.; Ramos, A.; Hernández, L.; Arévalo, L. C.; Pastor, E.; Louarn, G. *Int. J. Electrochem. Sci.* **2013**, *8*, 4120.

(14) Radisic, A.; Vereecken, P. M.; Hannon, J. B.; Searson, P. C.; Ross, F. M. *Nano Lett.* **2006**, *6*, 238.

(15) White, E. R.; Singer, S. B.; Augustyn, V.; Hubbard, W. A.; Mecklenburg, M.; Dunn, B.; Regan, B. C. *ACS Nano* **2012**, *6*, 6308.

(16) Sacci, R. L.; Dudney, N. J.; More, K. L.; Parent, L. R.; Arslan, I.; Browning, N. D.; Unocic, R. R. *Chem. Commun.* **2014**, *50*, 2104.

(17) Liao, J.; Martin, D. C. *Science* **1993**, *260*, 1489.

(18) Schneider, N. M.; Norton, M. M.; Mendel, B. J.; Grogan, J. M.; Ross, F. M.; Bau, H. H. *J. Phys. Chem. C* **2014**, *118*, 22373.

(19) Sutter, E. A.; Sutter, P. W. *J. Am. Chem. Soc.* **2014**, *136*, 16865.

(20) Patterson, J. P.; Abellan, P.; Park, C.; Browning, N. D.; Cohen, S. M.; Evans, J. E.; Gianneschi, N. C. *J. Am. Chem. Soc.* **2015**, *137*, 7322.

(21) Liao, H.; Zheng, H. *J. Am. Chem. Soc.* **2013**, *135*, 5038.

(22) Groenendaal, L.; Jonas, F.; Freitag, D.; Pielartzik, H.; Reynolds, J. R. *Adv. Mater.* **2000**, *12*, 481.

(23) Unocic, R. R.; Sun, X.-G.; Sacci, R. L.; Adamczyk, L. A.; Alsem, D. H.; Dai, S.; Dudney, N. J.; More, K. L. *Microsc. Microanal.* **2014**, *20*, 1029.

(24) Castagnola, V.; Bayon, C.; Descamps, E.; Bergaud, C. *Synth. Met.* **2014**, *189*, 7.

(25) Cui, X. T.; Zhou, D. D. *IEEE Trans. Neural Syst. Rehab. Eng.* **2007**, *15*, 502.

(26) Ahmad, S.; Carstens, T.; Berger, R.; Butt, H.-J.; Endres, F. *Nanoscale* **2011**, *3*, 251.

(27) Zheng, W.; Razal, J. M.; Spinks, G. M.; Truong, V. T.; Whitten, P. G.; Wallace, G. G. *Langmuir* **2012**, *28*, 10891.